Effect of Temperature, Composition, and Shear Rate on Polyvinylidene Fluoride/Dimethylacetamide Solution Viscosity

Nayef M. Ghasem,* Mohamed H. Al-Marzouqi, and Muftah H. El-Naas

Department of Chemical & Petroleum Engineering, UAE University, Al-Ain, P.O. Box 17555, U.A.E

Viscosity required for casting or spinning dope polymeric solution plays an essential role in the formulation of flat sheets and hollow fiber membranes. A flat sheet membrane can be casted from a polymer dope with viscosity as low as a few hundred centipoises; by contrast, a few thousand are required to spin polymeric hollow fibers. In this study, an empirical correlation describing the effect of temperature, polymer mass fraction, and shear rates on the viscosity of polyvinylidene fluoride polymer in dimethylacetamide solvent was derived. The dope polymer was used in the fabrication of polymeric hollow fiber membranes engaged in building membrane contactors for water treatment and the removal of carbon dioxide from natural gas. Data were obtained for (0.10, 0.15, 0.20, and 0.25) mass fraction of polyvinylidene fluoride in dimethylacetamide solvent at temperatures of (25, 35, 45, 55, 65, and 80) °C. The predicted values by the correlation were in good agreement with the experimental data. This empirical correlation accounts for temperature dependencies in the power law shear-thinning exponent. The correlation was derived using a nonlinear regression technique and statistical analysis software.

Introduction

Fluids are usually classified based on their behavior between shear stress and shear rate into Newtonian and non-Newtonian. Newtonian fluids are defined as those exhibiting a direct proportionality relationship between shear stress and shear rate, whereas for non-Newtonian fluids, the relationship between shear stress and shear rate is not linear. Pseudoplastic fluids are called shear thinning fluids because their apparent viscosity decreases with shear rate. Increasing shear breaks down the internal structure within the fluid very rapidly and reversibly, and no time dependence is manifested. The power law is a model for the shear dependency of the viscosities of polymer melts and solutions.

$$\tau = K\dot{\gamma}^n \tag{1}$$

Viscosity, η, is the ratio of shear stress to shear rate, hence

$$\eta = \tau/\dot{\gamma} \tag{2}$$

where τ is the shear stress; $\dot{\gamma}$ is the shear rate; and K and n are fitted parameters. The power law is accurate for the prediction of various viscosity shear rates for molten polymers.[1] It may be deduced that the applicability of the power law gets better with increasing solution concentration. If $n = 1$, the flow is Newtonian, and the viscosity does not change with shear rate. The flow is pseudoplastic or shear thinning if $n < 1$. Most polymer melts and solutions are pseudoplastic. The flow is dilatants or shear-thickening if $n > 1$. At very low or very high shear rates, Newtonian flow prevails. The melt or solution viscosity is constant; therefore, the power law applies only at intermediate rates of shear. If the polymer molecules are rigid rods or dumbbells which orient themselves in response to the shear forces, the dependence of viscosity on shear rate results from the extra molecular alignment that comes with each increase in shear rate.[2] At very low shear rates, the molecular orientation is random, and therefore, the viscosity is shearing independent. Molecular orientation does not occur below a threshold shear rate. At extremely high shear rates, the alignment process is complete, and additional shear makes no difference. The Andrade equation[3] describes the temperature reliance of liquid viscosities.

$$\eta = A_1 e^{C/T} \tag{3}$$

where η is viscosity in Pa and A_1 and C are fitted parameters. Viscosity also increases with increasing polymer concentration in exponential form

$$\eta = A_2 e^{DW} \tag{4}$$

where A_2 and D are fitted parameters while W is the polymer mass fraction. The above equations (eqs 1, 3, and 4) can be combined to study the effect of polymer melts and solution viscosities as a function of shear rates, temperature, and polymer concentrations

$$\tau = (K{\cdot}A_1{\cdot}A_2)\dot{\gamma}^n e^{C/T} e^{DW} \tag{5}$$

Combining the empirical constant of eq 5 leads to

$$\tau = A\dot{\gamma}^n e^{C/T} e^{DW} \tag{6}$$

The effect of temperature and shear rate on a polyisoimide solution viscosity was investigated.[4] Data were obtained for 0.20, 0.30, and 0.40 mass fraction polyisoimide solutions in the ratio of 20:80 tetrahydrofuran/diglyme and for a 0.30 mass fraction solution in *N*-methyl-pyrrolidone at temperatures of (25, 35, 55, and 75) °C. The measurements were taken on a Brookfield cone and plate viscometer at shear rates ranging from (9.59 to 383.4) reciprocal seconds. Experimental data fits proposed model reasonably well. In some cases, the model provides a better fit. This model accounts for temperature dependencies in the power law shear-thinning exponent. The coefficients depend on the material lot that is being tested even

* Corresponding author. E-mail: nayef@uaeu.ac.ae.

10.1021/je900248a CCC: $40.75
Published on Web 07/31/2009

Table 1. Properties of PVDF

property	unit	value
appearance	white	C
density	$g \cdot cm^{-3}$	1.78
volatile content	0.01	0.09
melt flow index @230 °C/2.16 kg	g/10 min	1.3
melting point	°C	170.5
particle size D 50	μm	90.9
intrinsic viscosity in DMF at 25 °C	g^{-1}	0.219
number average molecular weight		190 000
weight average molecular weight		304 000
polydispersity		1.6

though the molecular weights are very close. Slight differences in acid functional group concentrations for this particular material are a possible explanation. The effects of polymer concentration, temperature, and surfactant on the rheological properties of poly(*N*-isopropylacrylamide) and polyNIPAM were studied.[5] Below 28 °C, the viscosity decreased with increasing temperature according to the Arrhenius expression. However, at 29 °C, the viscosity increased to a maximum value at 32 °C, the lower critical solution temperature (LCST) for aqueous polyNIPAM. Higher temperatures gave much lower viscosity. This unusual rheological behavior was explained by the phase behavior of the polymer. Sodium dodecyl sulfate (SDS) binding to polyNIPAM increased the cloud point temperature (CPT) and attenuated the unusual rheological behavior of polyNIPAM in water. Rheological properties of carboxymethyl cellulose and κ-carrageenan mixtures have been studied. The influence of shear rate has been determined on different polymer ratios in aqueous solutions, upon the relative viscosity. The important effect caused by temperature on rheological behavior has also been studied. Characteristic behaviors were found for the mixtures analyzed, with clear deviations from linear trends that involve the existence of interactions between polymers. Models based on the viscosity of individual polymer solutions have been employed to analyze the experimental results.[6−9]

Recently, membrane ultrafiltration has been renowned as an efficient technique in the water purification process. Membrane filtrations are simple to operate, and in comparison with conventional water treatment methods, the energy required for operation and maintenance is low. It is a promising technology for purification and production of drinking water. Membrane filtration methods are capable of disinfecting water and removing its turbidity at moderately low pressure. Another advantage of membrane filtrations is the capability of removing a broad range of substances and the production of stable quality water. Membrane systems tend to be more compact.[10−12]

The prime objectives of the present work are to experimentally explore the effect of temperature, polymer mass fraction, and shear rates on the viscosity of polyvinylidene fluoride (PVDF) in dimethylacetamide (DMAc) solvent and to develop an empirical correlation to predict the experimental data. The empirical correlation can be used to predict the viscosity for polymer concentrations and temperatures that have not been experimentally studied and are within the acceptable correlation range.

Experimental Section

Polyvinylidene fluoride (PVDF) Solef 6020/1001 polymer was purchased from Solvay, France (Table 1). The solvent, dimethylacetamide (DMAc), was purchased from WAKO Chemicals, Japan. Four different concentrations of PVDF/DMAc were prepared, (0.10, 0.15, 0.20, and 0.25) mass fraction PVDF. Each solution was mixed for 24 h using a magnetic stirrer to ensure the solutions are homogeneous and perfectly mixed. Rheolab QC from Anton Paar, Austria, was used to measure the shear stress and viscosity of the polymer solutions versus shear rate for temperatures (25 to 80) °C, the same range of temperatures used in the preparation of the polymeric hollow fiber membrane utilizing nonsolvent-induced face separation techniques. The experimental data obtained for viscosity as a function of PVDF mass fraction, temperature, and shear rate are shown in Table 4.

Table 2. Parameter Estimates

		95 % confidence interval	
parameter	estimated value	lower limit	upper limit
A/Pa	3.79	−	−
B/s^{-1}	423041	346055	500027
n	1.283	1.28	1.30
C/K	2087	2063	2111
D	0.29	0.28	0.30

Table 3. Asymptotic Correlation Matrix of Parameters

	A/Pa	B/s^{-1}	n	C/K	D
A/Pa	−				
B/s^{-1}	−	1.00			
n	−	0.11	1.00		
C/K	−	0.53	−0.10	1.00	
D	−	0.77	−0.27	0.02	1.00

Results and Discussion

Most of the equations which describe the relationship between the shear stress and shear rate are empirical correlations. The two-parameter power law model ($\tau = K\dot{\gamma}^n$) is the most commonly used empirical equation for pseudoplastic fluids. In the present work, a more comprehensive model adopted from the parabolic shape is used in fitting the experimental data.

$$\tau = A[(1 + B^{-1}\dot{\gamma})^m - 1]^{m^{-1}} e^{CT^{-1}} e^{D(100 \cdot W)} \quad (7)$$

where A/Pa, B/s^{-1}, C/K, D, and m are empirical parameters; τ is the shear stress (Pa); $\dot{\gamma}$ is the shear rate (s^{-1}); T is the temperature in degree Kelvin; and W is the mass fractions of PVDF in DMAc solvent. The empirical parameters are obtained by fitting the experimental data with the proposed model. The fitted empirical constants were calculated using the Eazy-Fit software package,[13] and the results are shown in Table 2. The estimated parameters are within the 95 % confidence interval lower and upper limits. The obtained R^2 values were relatively high (above 0.99). The asymptotic correlation matrix of parameters is shown in Table 3. The results revealed that the parameters were independent except parameter A, which showed some dependency on B. Dividing both sides of the developed correlation by shear rate and rearranging leads to the following equations

$$\eta = A\dot{\gamma}^{-1}\{(1 + B^{-1}\dot{\gamma})^m - 1\}^{m^{-1}} e^{(C+100DW)T^{-1}} \quad (8)$$

Figures 1, 2, 3, and 4 show the viscosity versus shear rate for 0.25, 0.20, 0.15, and 0.10 mass fraction of PVDF, respectively. The plots show that the viscosity decreases with increasing shear. At a specific shear rate, the viscosity was found to increase exponentially with increasing polymer concentration (Figure 5). The effect of temperature on the apparent viscosity is shown in Figure 6, and the figure shows that the viscosity decreases with the increasing temperature. Polymer mixtures between (0.25 and 0.15) mass fraction PVDF show acceptable results between predicted and experimental data; by contrast, there is inconsistency between predicted viscosity and experimental data mainly for 0.10 mass fractions PVDF. At this low mass fraction,

Table 4. Viscosity, η, vs Shear Rate, $\dot{\gamma}$, at Different Temperatures and PVDF Mass Fraction, w

		η/Pa·s					
100w	$\dot{\gamma}$/s^{-1}	25 °C	35 °C	45 °C	55 °C	65 °C	80 °C
25	1.73	50.6	41.0	32.2	25.6	21.0	15.5
	3.45	47.6	39.2	31.3	25.1	20.8	15.5
	5.17	45.2	37.5	30.1	24.4	20.3	15.3
	6.90	43.0	35.9	29.1	23.7	19.9	15.0
	8.62	41.3	34.7	28.2	23.1	19.4	14.8
	10.3	39.8	33.5	27.4	22.6	19.0	14.5
	12.1	38.5	32.5	26.7	22.1	18.6	14.3
	13.8	37.3	31.6	26.0	21.6	18.2	14.1
	15.5	36.2	30.8	25.4	21.2	17.9	13.8
	17.2	35.3	30.1	24.9	20.8	17.6	13.6
	19.0	34.3	29.4	24.3	20.4	17.3	13.4
	20.7	33.5	28.8	23.9	20.1	17.0	13.3
	22.4	32.8	28.2	23.4	19.7	16.7	13.1
	24.1	32.0	27.6	23.0	19.4	16.5	12.9
	25.9	31.4	27.1	22.6	19.1	16.2	12.8
	27.6	30.7	26.6	22.2	18.9	16.0	12.6
	29.3	30.2	26.2	21.9	18.6	15.8	12.5
	31.0	29.6	25.7	21.6	18.4	15.6	12.3
	32.8	29.1	25.3	21.2	18.1	15.4	12.2
	34.5	28.6	24.9	20.9	17.9	15.2	12.1
	36.2	28.1	24.5	20.7	17.7	15.0	12.0
	37.9	27.6	24.2	20.4	17.5	14.8	11.8
	39.7	27.2	23.8	20.1	17.3	14.7	11.7
	41.4	26.8	23.5	19.8	17.1	14.5	11.6
	43.1	26.3	23.2	19.6	16.9	14.3	11.5
	44.8	26.0	22.8	19.4	16.7	14.2	11.4
	46.6	25.6	22.5	19.1	16.5	14.0	11.3
	48.3	25.2	22.3	18.9	16.3	13.9	11.2
	50.0	24.9	22.0	18.7	16.2	13.8	11.1
20	1.73	50.6	41.0	32.2	25.6	21.0	15.5
	3.45	47.6	39.2	31.3	25.1	20.8	15.5
	5.17	45.2	37.5	30.1	24.4	20.3	15.3
	6.9	43.0	35.9	29.1	23.7	19.9	15.0
	8.62	41.3	34.7	28.2	23.1	19.4	14.8
	10.3	39.8	33.5	27.4	22.6	19.0	14.5
	12.1	38.5	32.5	26.7	22.1	18.6	14.3
	13.8	37.3	31.6	26.0	21.6	18.2	14.1
	15.5	36.2	30.8	25.4	21.2	17.9	13.8
	17.2	35.3	30.1	24.9	20.8	17.6	13.6
	19.0	34.3	29.4	24.3	20.4	17.3	13.4
	20.7	33.5	28.8	23.9	20.1	17.0	13.3
	22.4	32.8	28.2	23.4	19.7	16.7	13.1
	24.1	32.0	27.6	23.0	19.4	16.5	12.9
	25.9	31.4	27.1	22.6	19.1	16.2	12.8
	27.6	30.7	26.6	22.2	18.9	16.0	12.6
	29.3	30.2	26.2	21.9	18.6	15.8	12.5
	31.0	29.6	25.7	21.6	18.4	15.6	12.3
	32.8	29.1	25.3	21.2	18.1	15.4	12.2
	34.5	28.6	24.9	20.9	17.9	15.2	12.1
	36.2	28.1	24.5	20.7	17.7	15.0	12.0
	37.9	27.6	24.2	20.4	17.5	14.8	11.8
	39.7	27.2	23.8	20.1	17.3	14.7	11.7
	41.4	26.8	23.5	19.8	17.1	14.5	11.6
	43.1	26.3	23.2	19.6	16.9	14.3	11.5
	44.8	26.0	22.8	19.4	16.7	14.2	11.4
	46.6	25.6	22.5	19.1	16.5	14.0	11.3
	48.3	25.2	22.3	18.9	16.3	13.9	11.2
	50.0	24.9	22.0	18.7	16.2	13.8	11.1
15	35	7.31	6.21	4.78	4.02	3.35	2.48
	69	6.35	5.24	4.02	3.49	2.93	2.12
	104	5.60	4.50	3.67	3.20	2.52	1.90
	138	5.30	4.22	3.45	2.95	2.43	1.72
	172	5.02	4.00	3.30	2.69	2.23	1.58
	207	4.76	3.82	3.13	2.57	2.11	1.56
	241	4.61	3.65	3.00	2.40	2.02	1.45
	276	4.42	3.60	2.90	2.40	1.99	1.35
	310	4.31	3.45	2.81	2.30	1.91	1.39
	345	4.26	3.42	2.76	2.22	1.80	1.28
	379	4.15	3.30	2.70	2.20	1.71	1.25

Table 4. Continued

		η/Pa·s					
100w	$\dot{\gamma}$/s^{-1}	25 °C	35 °C	45 °C	55 °C	65 °C	80 °C
10	35	1.470	1.180	1.010	0.838	0.807	0.708
	69	1.380	1.130	0.966	0.805	0.796	0.690
	104	1.300	1.080	0.928	0.782	0.78	0.672
	138	1.240	1.030	0.894	0.756	0.756	0.652
	172	1.180	0.993	0.864	0.735	0.736	0.635
	207	1.140	0.959	0.838	0.716	0.717	0.618
	241	1.100	0.928	0.814	0.698	0.699	0.603
	276	1.060	0.900	0.792	0.681	0.681	0.589
	310	1.030	0.875	0.772	0.666	0.665	0.577
	345	0.998	0.853	0.753	0.652	0.651	0.567
	379	0.971	0.832	0.737	0.639	0.638	0.557
	414	0.946	0.813	0.721	0.627	0.626	0.547
	448	0.923	0.795	0.706	0.615	0.614	0.539
	483	0.902	0.778	0.693	0.604	0.603	0.531
	517	0.882	0.763	0.680	0.595	0.593	0.523
	552	0.864	0.748	0.668	0.585	0.584	0.516
	586	0.846	0.735	0.657	0.576	0.574	0.509
	621	0.830	0.723	0.647	0.568	0.566	0.503
	655	0.815	0.710	0.636	0.560	0.558	0.497
	690	0.800	0.699	0.627	0.552	0.55	0.491
	724	0.787	0.688	0.618	0.545	0.543	0.486
	759	0.773	0.678	0.609	0.538	0.536	0.481
	793	0.761	0.668	0.601	0.531	0.529	0.477
	828	0.749	0.659	0.593	0.525	0.523	0.473
	862	0.738	0.65	0.585	0.519	0.517	0.469
	897	0.727	0.641	0.578	0.513	0.511	0.464
	931	0.717	0.633	0.571	0.508	0.506	0.461
	966	0.707	0.625	0.565	0.502	0.501	0.458
	1000	0.698	0.618	0.558	0.497	0.496	0.454

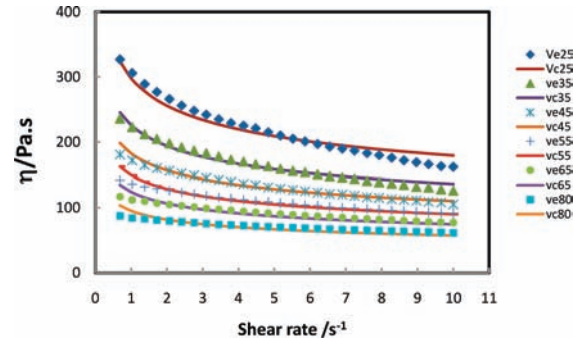

Figure 1. Viscosity vs shear rate for 0.25 mass fractions PVDF. vc, calculated viscosity; and ve, experimental viscosity.

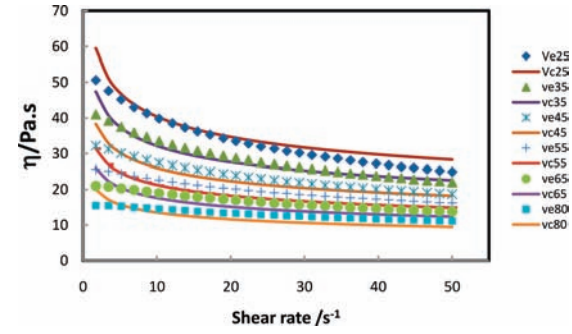

Figure 2. Viscosity vs shear rate for 0.20 mass fractions PVDF. vc, calculated viscosity; and ve, experimental viscosity.

viscosity is almost constant (Newtonian behavior). The figures indicate that the viscosity increases with the increasing PVDF mass fraction and decreasing temperature. The fractional deviation between experimental and calculated viscosities versus shear rate/maximum shear rate is shown in Figure 7. The plot shows that the deviation between predicted and experimental values is high at very low shear rate (less than 12 s^{-1}). By contrast,

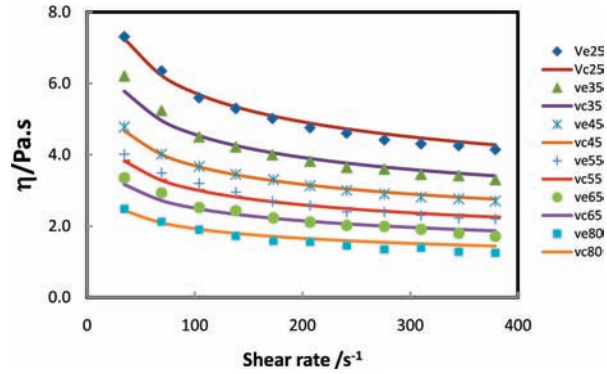

Figure 3. Viscosity vs shear rate for 0.15 mass fractions PVDF. vc, calculated viscosity; and ve, experimental viscosity.

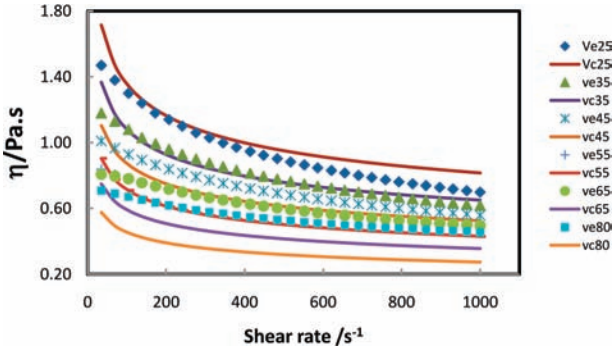

Figure 4. Viscosity vs shear rate for 0.10 mass fractions PVDF. vc, calculated viscosity; and ve, experimental viscosity.

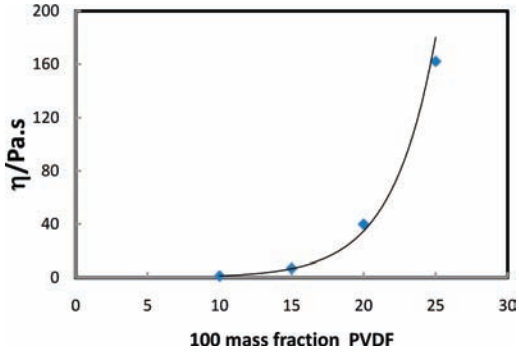

Figure 5. Viscosity vs 100 mass fractions PVDF at fixed shear rate.

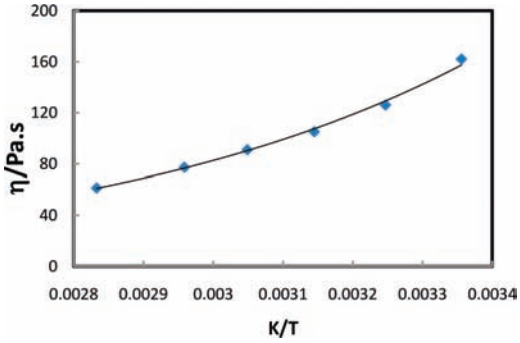

Figure 6. Viscosity vs temperature for 0.25 mass fraction PVDF and fixed shear rate.

the divergence decreases with increasing shear rate. The adequate range of shear rate is (12 to 1000) s^{-1} as shown in Figure 8. Figure 8 was plotted in this shear rate range, and hence the discrepancy between experimental and predicted data was insignificant.

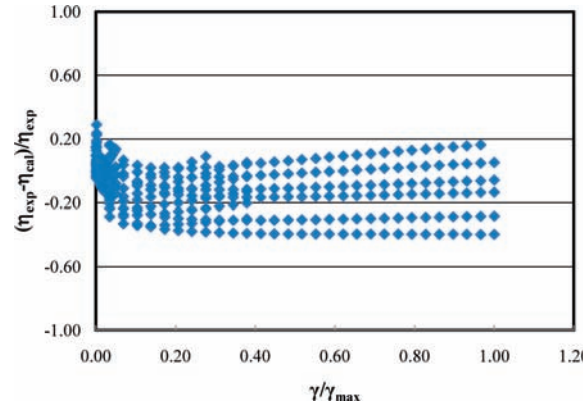

Figure 7. Fractional deviation between experimental (η_{exp}) and calculated (η_{calc}) viscosity versus shear rate/max shear rate.

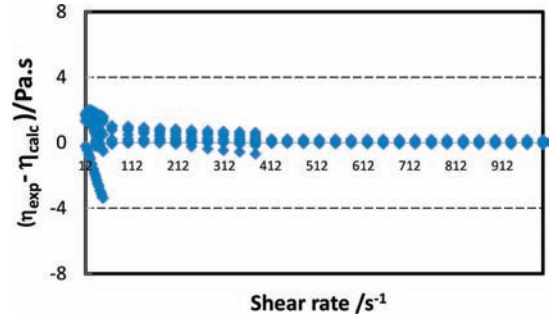

Figure 8. Deviation between experimental (η_{exp}) and calculated (η_{calc}) viscosity for shear rates in the range (12 to 1000) s^{-1}.

Conclusions

A generalized rheological model was developed for the prediction of viscosity vs shear rate for four different PVDF/DMAc mass fractions and six different temperatures. This polymeric solution is frequently used in the fabrication of a hollow fiber membrane using the nonsolvent-induced phase separation (NIPS) process. The generated empirical correlation was found to successfully correlate the viscosity to the shear rate for the shear rate range (12 to 1000) s^{-1} and PVDF mass fraction range (0.15 to 0.25). This range of mass fractions is the most suitable for the fabrication of polymeric hollow fiber membranes. For PVDF mass fraction of 0.10, the discrepancy is due to the Newtonian behavior of this solution, mainly at high shear rate, in which viscosity does not change with changing shear rate. In general, the PVDF/DMAc polymeric solution behaves as pseudoplastic fluids, where the apparent viscosity decreases instantaneously with an increase in shear rate and temperature; by contrast, it increases with the increasing polymer mass fraction.

Literature Cited

(1) Rodriguesz, F. *Principles of Polymer Systems*; McGraw-Hill, 1970.
(2) Bird, R. B.; Hassager, O; Armstrong, R. C.; Curtiss, C. F. *Dynamics of Polymeric Liquids*; John Wiley & Sons, 1977.
(3) Murrell, H. N.; Boucher, E. A. *Properties of Liquids and Solutions*; John Wiley & Sons, 1982.
(4) Levinso, W.; Czornyj, G.; Capo, D.; McMahon, J. Effect of temperature and shear rate on polyisoimide solution viscosity. *Polym. Eng. Sci.* **2004**, *18*, 1221–1225.
(5) Tam, K. C.; Wu, X. Y.; Pelton, R. H. Effect of Polymer Concentration, Temperature, and Surfactant on the Viscosity of Aqueous Solutions. *J. Polym. Sci. Part A: Polym. Chem.* **2003**, *31*, 963–969.
(6) Gómez-Díaz, D.; Navaza, J.; Quintáns-Riveiro, L. Influence of Mixing and Temperature on the Rheological Properties of Carboxymethyl Cellulose/κ-carrageenan Mixtures. *Eur. Food Res. Technol.* **2008**, *5*, 1397–1402.

(7) Atchariyawuta, S.; Jiraratananona, R.; Wang, R. Mass Transfer Study and Modeling of Gas-liquid Membrane Contacting Process by Multistage Cascade Model for CO_2 absorption. *Sep. Purif. Technol.* **2008**, *63*, 15–22.

(8) Dan-ying, Z.; You-yi, X.; Han-tao, Z. The Influence of PEG Molecular Weight on Morphologies and Properties of PVDF Asymmetric Membranes. *Chin. J. Polym. Sci.* **2008**, *26*, 405–414.

(9) Byoung, H. K.; Byoung, C. The Rheological Properties of the Solutions of PVDF in DMAc for Electrospinning. *Korean Fiber Soc.* **2004**, *41*, 419–423.

(10) Jermann, D.; Pronk, W.; Meylan, S.; Boller, M. Interplay of different NOM fouling mechanisms during ultrafiltration for drinking water production. *Water Res.* **2007**, *41*, 1713–1722.

(11) Madaeni, S. S. The application of membrane technology for water disinfection. *Water Res.* **1999**, *33*, 301–308.

(12) Pearce, G. Introduction to membranes: Filtration for water and wastewater treatment. *Filtr. Sep.* **2007**, *44*, 24–27.

(13) Schittkowski, K. *EASY-FIT User Guide*; Department of Mathematics, University of Bayreuth: Germany, 2008.

Received for review March 08, 2009. Accepted July 21, 2009. The authors would like to acknowledge the financial support provided by the Japan Cooperation Center, Petroleum (JCCP), and the technical support of the Nippon Oil Research Institute Co., Ltd. (NORI). They would also like to thank ADGAS and UAEU Research Affairs for their support.

JE900248A